
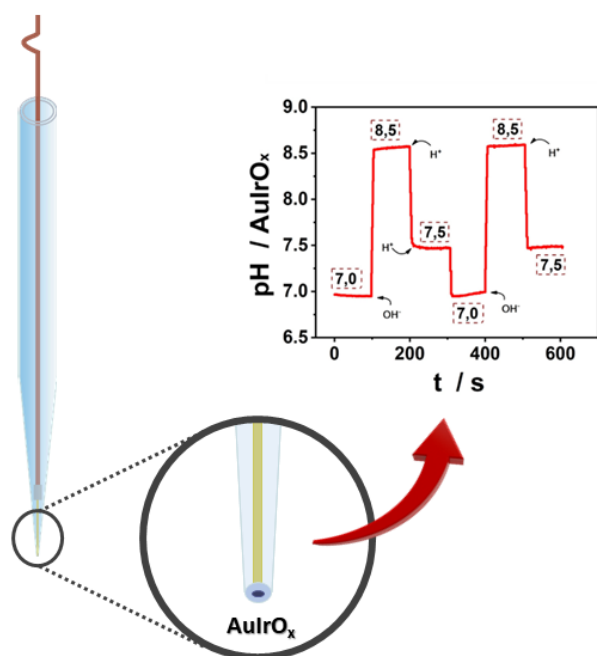


ARTICLE

Iridium Oxides Based Potentiometric Sensor for pH Monitoring in Biological Samples

Jessica Soares Guimaraes Selva^{id}, Mauro Bertotti^{*id} 

Departamento de Química Fundamental, Instituto de Química, Universidade de São Paulo, Av. Professor Lineu Prestes, 748, 05508-000, São Paulo, SP, Brazil



The fabrication and long-term application of a pH Au microelectrode based on an iridium oxide film are reported. A uniform iridium oxide film with a typical thickness of around 1 μm was coated on the microelectrode surface through a 2-step procedure involving electrodeposition at constant potential and further continuous voltammetric scans. A super-Nernstian slope of around 77 mV per pH unit was found from open circuit potential measurements in a broad pH range (2 to 10) in 0.01 mol L⁻¹ phosphate buffer. It was demonstrated experimentally that the short-term pH precision of the IrO_x sensor is ± 0.1 pH. The response stability was maintained in the physiological pH range, and the sensor exhibited excellent reproducibility, long-term stability, and a short response time of < 10 s. The results reported in this work confirmed that iridium oxide showed very promising pH sensing performance and can serve as an electrode material for detecting local pH changes in samples of increased complexity, such as juice fruits, culture medium, synthetic urine, and blood.

Keywords: Potentiometric sensor, iridium oxides, pH sensor, microelectrodes, biological samples

INTRODUCTION

The original glass electrode probe is the most employed sensor for pH measurements because of its reliability, accuracy, and lifetime. However, there is a continuous interest in developing pH sensors on a miniature scale. Accordingly, efforts have been devoted in the last years to fabricate pH sensors that are relatively easy to miniaturize by using several solid-state metal oxides, including PtO₂, IrO_x, RuO₂, OsO₂, Ta₂O₅, RhO₂, TiO₂, and SnO₂.¹

Iridium oxide (IrO_x)-modified electrodes have received particular attention, mainly for applications towards sensing different molecules of biological relevance.² Such material has also been extensively used in fabricating potentiometric pH sensors because of the formation of hydroxide groups on the oxide

Cite: Selva, J. S. G.; Bertotti, M. Iridium Oxides Based Potentiometric Sensor for pH Monitoring in Biological Samples. *Braz. J. Anal. Chem.* 2023, 10 (40), pp 90-98. <http://dx.doi.org/10.30744/brjac.2179-3425.AR-108-2022>

Submitted 09 November 2022, Resubmitted 23 January 2023, Accepted 01 March 2023, Available online 17 March 2023.

surface. The potential of the interface is determined by the ratio of the Ir(III) and Ir(IV) species, which in turn depends on the proton exchange capacity facilitated by the OH⁻ groups on the surface.^{3,4}

pH potentiometric sensors based on IrO_x films are quite attractive because they present some interesting features such as potential stability, relationship between potential and pH over a wide range, fast response, and response immunity from the interference of redox species.⁵⁻⁸ The pH sensing using iridium oxide materials has mainly been explored in different fields, i.e., to get information on pH in biological medium and corrosion studies, as well as for *in situ* measurements and in microscopic environments.⁹⁻¹⁸

The electrodeposition of iridium oxide films onto electrode surfaces has been conducted by different approaches. Among them, galvanostatic deposition proved to be the least indicated since it can provide fragile films which can be easily damaged. Potentiostatic electrodeposition provides more reproducible films, but they remain brittle. Elsen *et al.*¹⁹ observed that films produced by cyclic voltammetry and constant applied potential are more compact and durable. Santos *et al.*¹⁵ reported that more robust and reproducible iridium oxide films were obtained through a two-step procedure based on potentiostatic polarization for a certain time and subsequent recording of a few voltammetric cycles.

In previous work, we have fabricated a miniaturized Au microelectrode containing an iridium oxide film to get information on the role of transporters and pumps in larva midgut through pH determinations.²⁰ Our goal now is to enhance some features of such a microsensor aiming at getting more sensitive pH measurements with enhanced stability and short response time. This was achieved by changing some conditions in the protocol employed for the film preparation. We have demonstrated that such a miniaturized sensor shows favorable sensing performance and can be successfully applied to measure pH in biological samples.

MATERIALS AND METHODS

Chemicals

All chemicals and reagents were analytical grade and used without any further purification. All aqueous solutions were prepared using ultrapure water (Barnstead Nanopure Systems, 18 MΩ cm).

Instrumentation

The electrochemical experiments were performed using an Autolab PGSTAT128 potentiostat (Metrohm, Utrecht, Netherlands), interfaced with NOVA 1.11 software for data acquisition. Cyclic voltammograms (CVs) were recorded in a three-electrode configuration, using a gold microelectrode, Ag|AgCl|KCl_(sat), and platinum wire as the working, reference, and auxiliary electrodes, respectively. Open circuit potential (OCP) measurements were conducted with the AulrO_x sensor as the indicator electrode and a Ag|AgCl|KCl_(sat) as the reference.

AulrO_x Sensor preparation

A AulrO_x sensor was manufactured from a gold microfiber (99.99%, hard, 0.025 mm, Goodfellow®) sealed into a borosilicate capillary (O.D. 1 mm, I.D. 0.5 mm e 10 cm long, Sutter Instrument Company®) using a micropipette puller P2000. An [Ir(COO)₂(OH)₄]²⁻ solution was used for the electrodeposition of the IrO_x film onto the electrode surface. The solution is prepared from [IrCl₆]²⁻, H₂O₂ 30% (w/w) and C₂H₂O₄, and the pH is adjusted to 10.5 using K₂CO₃, as previously reported by Santos¹⁵ and Yamanaka²¹. The electrodeposition was accomplished according to a 2-step procedure:

- i) A constant potential was applied for 600 s (0.8 V vs. Ag|AgCl|KCl_(sat)).
- ii) 50 voltammetric cycles were recorded at scan rate = 100 mV s⁻¹ from 0 to 1 V vs. Ag|AgCl|KCl_(sat),

The sensor's electrochemical behavior was examined through cyclic voltammetry in a 0.01 mol L⁻¹ phosphate buffer solution (pH 7.0), which was also employed to calibrate the the AulrO_x sensor at different pH values.

Biological application

The AulrO_x sensor was employed to follow pH changes through OCP measurements. Before use, the device was calibrated adequately in a phosphate buffer solution in a pH range from 2 to 10. The sensor was placed in the solution during the measurements, and the potential was recorded for 60 s. The pH of all samples was measured with a commercial glass electrode for comparison, except for the blood sample, whose pH was measured through the arterial blood gas technique.^{22,23}

RESULTS AND DISCUSSION

Figure 1 shows the CVs obtained after the potentiostatic step ($E = 0.8$ V vs. $\text{Ag}|\text{AgCl}|\text{KCl}_{(\text{sat})}$ for 600 s), where an IrO_x film was electrodeposited. In the forward scans the peaks around 0.4 V and 0.8 V correspond to the oxidation of Ir (II) to Ir (III) and then to Ir (IV), respectively. In the reverse scans, the peaks around 0.55 V and 0.3 V correspond to the inverse processes. The electron transfer processes involving the iridium oxides lead to a continuous current increase as a consequence of the material accumulated onto the electrode surface during the CVs recording. Such a procedure leads to the growth of a mixed film of Ir(IV)/Ir(III) oxides with greater crystallinity and stability, which is sensitive to changes in the pH.^{15,24} The number of potential cycles determines the amount of material electrodeposited on the electrode surface, as well as its distribution.

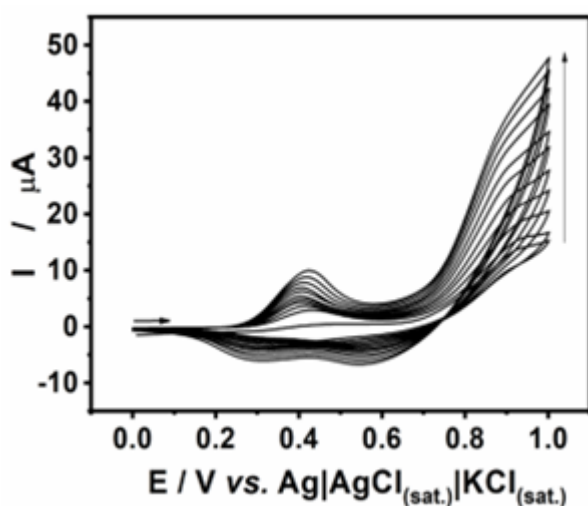
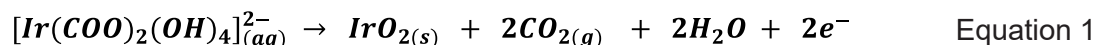


Figure 1. Cyclic voltammograms recorded with a Au microelectrode ($r = 2.5 \mu\text{m}$) in the iridium complex solution (pH 10.5) after the electrodeposition step. $v = 100 \text{ mV s}^{-1}$. Here are presented the first CV and, after that, one every five measurements.

Although the mechanism for the film formation is still not well established in the literature, the most accepted reaction can be described by Equation 1^{15,18,21}:



According to this reaction, the deposition of a hydrated iridium oxide film and the parallel formation of CO_2 take place.

To confirm the oxide layer electrodeposition, voltammograms were recorded in phosphate buffer solution (pH 7.0) before and after the 2-step procedure. By inspection of the CV shown in Figure 2 (red curve), the modification of the microelectrode surface is clearly confirmed. For instance, a voltammetric curve that resembles those obtained in a solution containing the iridium complex (Figure 1) is noticed in the 0.0 to 0.5 V potential range. Such electron transfer processes correspond to the Ir(III) oxide oxidation and concurrent reverse process (reduction of Ir(IV) oxide). The thickness of the film oxide layer was calculated by taking into account the charge under the cathodic peak and considering that a $1 \mu\text{m}$ thick iridium oxide film contains ca. $7.8 \times 10^{-7} \text{ mol cm}^{-2}$, hence the film thickness was found to be $0.91 \mu\text{m}$.¹⁵

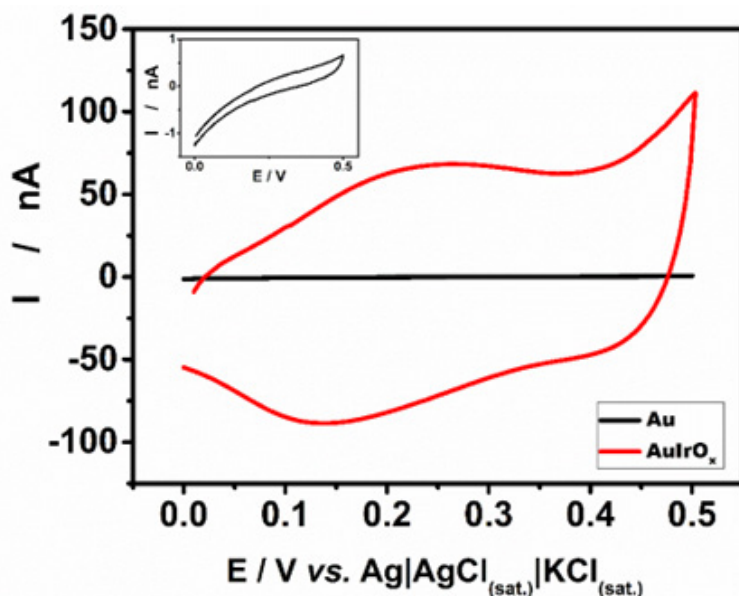
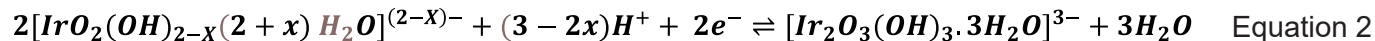


Figure 2. Cyclic voltammograms recorded in 0.01 mol L⁻¹ PBS (pH 7.0), before and after the gold surface modification. $\nu = 100 \text{ mV s}^{-1}$. Inset: Cyclic voltammogram recorded at the gold surface before the modification rescaled.

The sensitivity of the fabricated IrO_x sensor to pH was examined through open circuit potential measurements in 0.01 mol L⁻¹ phosphate solution at different pH values, and Figure 3 displays the results. A linear correlation between potential values and solution pH is observed, and this dependence is based on the electron transfer reaction that governs the pH-sensitive properties of the AulrO_x sensor, given by Equation 2:^{15,25,26}



Therefore, the redox potential can be expressed as indicated by Equation 3:

$$E = E^0 - \frac{2.303RT(3-2x)}{2F} \text{pH} = E^0 - \frac{59(3-2x)}{2} \text{pH} \quad \text{Equation 3}$$

where: E = redox potential (mV); E⁰ = standard electrode potential (mV); R = universal ideal gas constant (8.314 J K⁻¹ mol⁻¹); T = temperature (K); F = Faraday constant (96485 C mol⁻¹); x = a value between 0 and 2.¹⁸

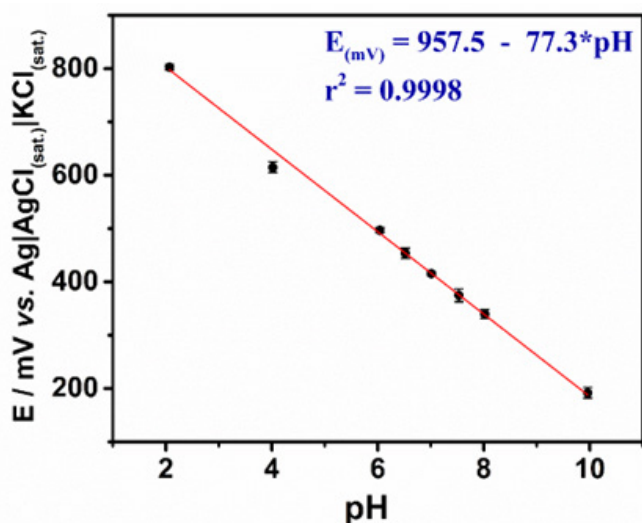


Figure 3. Potential values measured with the AulrO_x sensor as a function of pH.

It is easily deducible from Equation 3 that the slope value is 59 mV pH^{-1} when $x = 0.5$, the typical case where the number of electrons transferred in Equation 2 is equivalent to the number of protons. Likewise, for $x = 0$, the slope is 88.5 mV pH^{-1} , and a ratio of 3 protons to 2 electrons is expected. Hence, the difference in sensitivity is attributed to a mixed potential of two different oxyhydroxide states regarding the iridium oxide films.

A super-Nernstian response in an extensive pH range is exhibited in Figure 3. Such a behavior is usual for AulrO_x electrodes, for which slopes can vary up to $-90 \text{ mV per pH unit}$.^{15,27} The relative acidity of both iridium oxides involved in Equation 2^{28,29} determines the pH response and justifies slopes higher than $60 \text{ mV per pH unit}$.^{30,31}

A potentiometric titration was performed in order to evaluate the response time of the AulrO_x sensor to changes in pH, as well as the device's ability to detect slight variations in the solution pH. Measurements with the AulrO_x sensor were performed in the 6.5 to 7.5 pH range, and a parallel study was also conducted with a commercial pHmeter. Figure 4A displays the results, and one can conclude that the fabricated AulrO_x sensor responded quite adequately to changes in pH, providing quick and stable responses. Furthermore, the pH values provided by the AulrO_x sensor are in excellent agreement with those obtained with the pHmeter, as shown in Figure 4B.

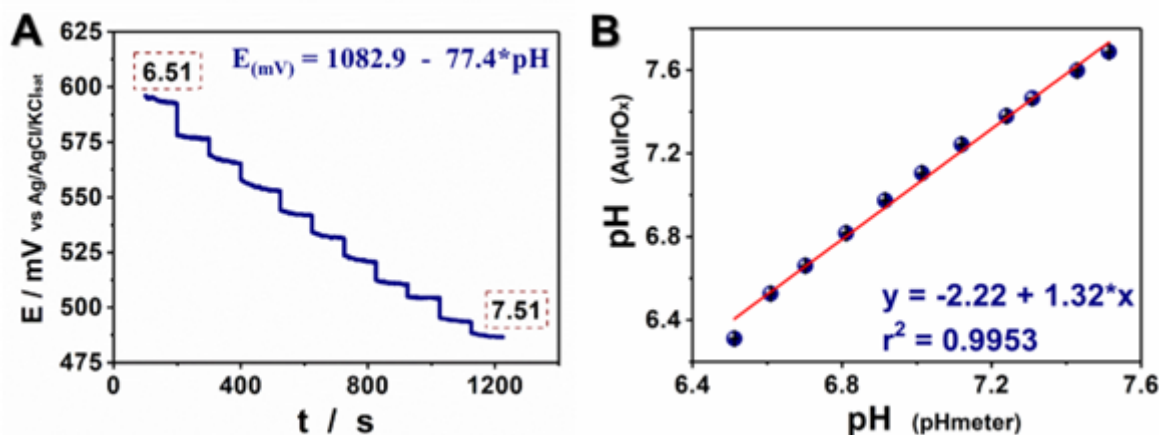


Figure 4. A) Dependence of OCP measurements recorded with the AulrO_x sensor on the pH. Values presented in the boxes correspond to those measured with the pHmeter. **B)** Correlation plot of pH values measured with the pHmeter and the AulrO_x sensor.

The fabricated sensor was applied to get the pH information in more complex samples such as synthetic urine, lemon juice, DMEM (Dulbecco's modified Eagle's medium), and blood. Table I shows that the AulrO_x sensor presented satisfactory results compared with the reference values. In order to check whether there was a difference between the results, a paired t test was performed, where it was found that there is no significant difference between the methods with a 95% confidence level.

Table I. Comparison between pH values of different samples measured with a glass electrode or by gasometry (blood) and those obtained with the AulrO_x sensor (n=3)

Sample	pH (Reference)	pH (AulrO_x Sensor)
Lemon juice	2.37	2.50 (± 0.08)
Synthetic urine	6.06	5.76 (± 0.02)
Synthetic urine + NaOH	6.73	6.38 (± 0.03)

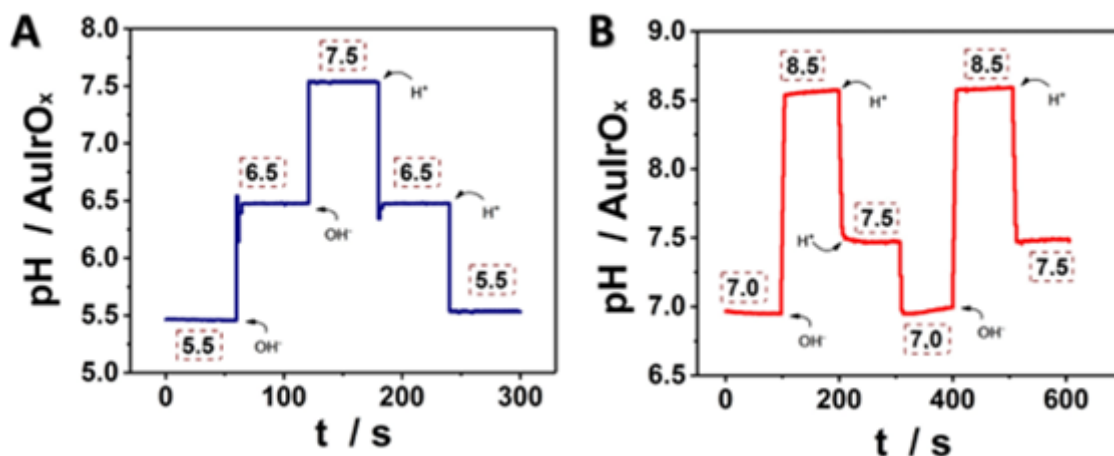
(continues on the next page)

Table I. Comparison between pH values of different samples measured with a glass electrode or by gasometry (blood) and those obtained with the AulrO_x sensor (n=3) (continuation)

Sample	pH (Reference)	pH (AulrO _x Sensor)
DMEM	8.49	8.76 (± 0.07)
DMEN + CH ₃ COOH	4.17	4.63 (± 0.09)
Blood	6.88	7.1 (± 0.1)

The response time of the proposed sensor was assessed through measurements in a complex sample matrix. Accordingly, a synthetic urine solution's pH was monitored after adding small volumes of 0.1 mol L⁻¹ NaOH and 0.5 mol L⁻¹ H₂SO₄ solutions. Measurements were performed under stirring using the AulrO_x sensor and a glass electrode during the entire process. A similar experiment was also performed using a DMEM solution, and Figure 5 presents the results. It is observed that, despite the slight difference between the absolute pH values, the sensor follows the solutions pH changes in both experiments. Moreover, no memory effect was observed, even in complex media such as synthetic urine and DMEM solution.

The results shown in Figure 5 also indicate that the response time of the AulrO_x sensor was very short. For instance, after adding acid or base solutions, a potential stabilization was achieved after around 5 s, which is considered relatively fast for pH sensing devices based on oxide films. In the literature,^{5,27,32,33} it appears that, on average, sensors based on electrodeposited iridium oxide films (EIROF's) exhibit response times greater than 10 s. This shows that the developed sensor is quite efficient for real-time pH monitoring.

**Figure 5.** pH monitoring obtained with the AulrO_x sensor in: **A)** synthetic urine; **B)** DMEM during addition of 0.1 mol L⁻¹ NaOH and 0.5 mol L⁻¹ H₂SO₄ solutions. The boxes show the pH values measured with the pHmeter.

CONCLUSIONS

By coating the surface of a Au microelectrode with a layer of IrO_x, a potentiometric pH sensor was fabricated. The film was electrodeposited from an iridium complex solution by applying 0.8 V vs. Ag|AgCl|KCl_(sat) for 600 s, followed by recording 50 cyclic voltammograms. This methodology allowed obtaining robust, stable, and sensitive IrO_x films to monitor reliably pH changes in solutions with a complex composition such as blood, synthetic urine, and DMEM culture medium. In addition, the device presented a wide working range (from pH 2 to 10) and fast response (< 10 s), allowing stable and sensitive pH measurements (0.1 unit).

In conclusion, the proposed AuIrO_x sensor showed extremely promising attributes for getting real-time pH, having the potential to be an important tool in the study of complex systems such as biological medium. It should also be pointed out that such a sensor can be easily miniaturized, hence chemical information can be obtained in microscopic environments such as single cells.

Conflicts of interest

There are not conflicts to declare.

Acknowledgements

The authors would like to thank the financial support from the São Paulo State Research Foundation (FAPESP 2018/08782-1), and the National Council for Scientific and Technological Development (CNPq 141866/2016-0).

REFERENCES

- (1) Manjakkal, L.; Szwagierczak, D.; Dahiya, R. Metal Oxides Based Electrochemical pH Sensors: Current Progress and Future Perspectives. *Prog. Mater. Sci.* **2020**, *109*, 100635. <https://doi.org/10.1016/j.pmatsci.2019.100635>
- (2) Dong, Q.; Sun, X.; He, S. Iridium Oxide Enabled Sensors Applications. *Catalysts* **2021**, *11* (10), 1164. <https://doi.org/10.3390/catal11101164>
- (3) Hitchman, M. L.; Ramanathan, S. Considerations of the pH Dependence of Hydrous Oxide Films Formed on Iridium by Voltammetric Cycling. *Electroanalysis* **1992**, *4* (3), 291–297. <https://doi.org/10.1002/elan.1140040306>
- (4) Olthuis, W.; Robben, M. A. M.; Bergveld, P.; Bos, M.; van der Linden, W. E. pH Sensor Properties of Electrochemically Grown Iridium Oxide. *Sens. Actuators, B* **1990**, *2* (4), 247–256. [https://doi.org/10.1016/0925-4005\(90\)80150-X](https://doi.org/10.1016/0925-4005(90)80150-X)
- (5) Marzouk, S. A. M.; Ufer, S.; Buck, R. P.; Johnson, T. A.; Dunlap, L. A.; Cascio, W. E. Electrodeposited Iridium Oxide pH Electrode for Measurement of Extracellular Myocardial Acidosis during Acute Ischemia. *Anal. Chem.* **1998**, *70* (23), 5054–5061. <https://doi.org/10.1021/ac980608e>
- (6) Papeschi, G.; Bordi, S.; Carla, M.; Criscione, L.; Ledda, F. An Iridium-Iridium Oxide Electrode for in Vivo Monitoring of Blood pH Changes. *J. Med. Eng. Technol.* **2009**, *5* (2), 86–87. <https://doi.org/10.3109/03091908109042445>
- (7) Fog, A. Electronic Semiconducting Oxides as pH Sensors. *Sens. Actuators* **1984**, *5*, 13–20.
- (8) Kinlen, P. J.; Heider, J. E.; Hubbard, D. E. A Solid-State pH Sensor Based on a Nafion-Coated Iridium Oxide Indicator Electrode and a Polymer-Based Silver Chloride Reference Electrode. *Sens. Actuators, B* **1994**, *22* (1), 13–25. [https://doi.org/10.1016/0925-4005\(94\)01254-7](https://doi.org/10.1016/0925-4005(94)01254-7)
- (9) O'Hare, D.; Parker, K. H.; Winlove, C. P. Metal-Metal Oxide pH Sensors for Physiological Application. *Med. Eng. Phys.* **2006**, *28* (10), 982–988. <https://doi.org/10.1016/j.medengphy.2006.05.003>
- (10) Gláb, S.; Hulanicki, A.; Edwall, G.; Folke, F.; Ingman, I.; Koch, W. F. Metal-Metal Oxide and Metal Oxide Electrodes as pH Sensors. *Crit. Rev. Anal. Chem.* **1989**. <https://doi.org/10.1080/10408348908048815>
- (11) Smiechowski, M. F.; Lvovich, V. F. Iridium Oxide Sensors for Acidity and Basicity Detection in Industrial Lubricants. *Sens. Actuators, B* **2003**, *96* (1–2), 261–267. [https://doi.org/10.1016/S0925-4005\(03\)00542-2](https://doi.org/10.1016/S0925-4005(03)00542-2)
- (12) Kakooei, S.; Ismaila, M. C.; Ari-Wahjoedia, B. Electrodeposition of Iridium Oxide by Cyclic Voltammetry: Application of Response Surface Methodology. *MATEC Web Conf.* **2014**, *13*, 04024. <https://doi.org/10.1051/mateconf/20141304024>
- (13) Nguyen, C. M.; Rao, S.; Seo, Y.-S.; Schadt, K.; Hao, Y.; Chiao, J.-C. Micro pH Sensors Based on Iridium Oxide Nanotubes. *IEEE Trans. Nanotechnol.* **2014**, *13* (5), 945–953. <https://doi.org/10.1109/TNANO.2014.2332871>

- (14) Yang, J.; Kwak, T. J.; Zhang, X.; McClain, R.; Chang, W. J.; Gunasekaran, S. Digital pH Test Strips for In-Field pH Monitoring Using Iridium Oxide-Reduced Graphene Oxide Hybrid Thin Films. *ACS Sens.* **2016**, 1 (10), 1235–1243. https://doi.org/10.1021/ACSSENSORS.6B00385/ASSET/IMAGES/SE-2016-00385M_M009.GIF
- (15) Santos, C. S.; Lima, A. S.; Battistel, D.; Daniele, S.; Bertotti, M. Fabrication and Use of Dual-Function Iridium Oxide Coated Gold SECM Tips. An application to pH Monitoring above a Copper Electrode Surface during Nitrate Reduction. *Electroanalysis* **2016**, 28 (7), 1441–1447. <https://doi.org/10.1002/elan.201501082>
- (16) Rouhi, J. Development of Iridium Oxide Sensor for Surface pH Measurement of a Corroding Metal under Deposit. *Int. J. Electrochem. Sci.* **2017**, 12, 9933–9943. <https://doi.org/10.20964/2017.11.07>
- (17) Jović, M.; Hidalgo-Acosta, J. C.; Lesch, A.; Costa Bassetto, V.; Smirnov, E.; Cortés-Salazar, F.; Girault, H. H. Large-Scale Layer-by-Layer Inkjet Printing of Flexible Iridium-Oxide Based pH Sensors. *J. Electroanal. Chem.* **2018**, 819, 384–390. <https://doi.org/10.1016/j.jelechem.2017.11.032>
- (18) Zhu, Z.; Liu, X.; Ye, Z.; Zhang, J.; Cao, F.; Zhang, J. A Fabrication of Iridium Oxide Film pH Micro-Sensor on Pt Ultramicroelectrode and Its Application on in-Situ pH Distribution of 316L Stainless Steel Corrosion at Open Circuit Potential. *Sens. Actuators B Chem* **2018**, 255, 1974–1982. <https://doi.org/10.1016/j.snb.2017.08.219>
- (19) Elsen, H. A. Thermodynamic and Dynamic Investigations of Hydrated Iridium Oxide Potentiometric pH Micro-Sensors. PhD thesis, University of California Berkeley, 2007.
- (20) Barroso, I. G.; Santos, C. S.; Bertotti, M.; Ferreira, C.; Terra, W. R. Molecular Mechanisms Associated with Acidification and Alkalization along the Larval Midgut of *Musca Domestica*. *Comp. Biochem. Physiol., Part A: Mol. Integr. Physiol.* **2019**, 237, 110535. <https://doi.org/10.1016/j.cbpa.2019.110535>
- (21) Yamanaka, K. Anodically Electrodeposited Iridium Oxide Films (AEIROF) from Alkaline Solutions for Electrochromic Display Devices. *Jpn. J. Appl. Phys.* **1989**, 28 (4R), 632–637. <https://doi.org/10.1143/JJAP.28.632>
- (22) Williams, A. J. Assessing and Interpreting Arterial Blood Gases and Acid-Base Balance. *BMJ* **1998**, 317, 1213–1216. <https://doi.org/10.1136/bmj.317.7167.1213>
- (23) Viegas, C. A. A. Gasometria arterial. *J. Pneumol.* **2002**, 28 (Supl3), S233–S238.
- (24) Steegstra, P.; Busch, M.; Panas, I.; Ahlberg, E. Revisiting the Redox Properties of Hydrous Iridium Oxide Films in the Context of Oxygen Evolution. *J. Phys. Chem. C* **2013**, 117 (40), 20975–20981. <https://doi.org/10.1021/jp407030r>
- (25) Baur, J. E.; Spaine, T. W. Electrochemical Deposition of Iridium (IV) Oxide from Alkaline Solutions of Iridium(III) Oxide. *J. Electroanal. Chem.* **1998**, 443 (2), 208–216. [https://doi.org/10.1016/S0022-0728\(97\)00532-9](https://doi.org/10.1016/S0022-0728(97)00532-9)
- (26) Burke, L. D.; Mulcahy, J. K.; Whelan, D. P. Preparation of an Oxidized Iridium Electrode and the Variation of Its Potential with pH. *J. Electroanal. Chem. Interfacial Electrochem.* **1984**, 163 (1–2), 117–128. [https://doi.org/10.1016/S0022-0728\(84\)80045-5](https://doi.org/10.1016/S0022-0728(84)80045-5)
- (27) Elsen, H. A.; Monson, C. F.; Majda, M. Effects of Electrodeposition Conditions and Protocol on the Properties of Iridium Oxide pH Sensor Electrodes. *J. Electrochem. Soc.* **2009**, 156 (1), F1–F6. <https://doi.org/10.1149/1.3001924>
- (28) Clausmeyer, J.; Masa, J.; Ventosa, E.; Öhl, D.; Schuhmann, W. Nanoelectrodes Reveal the Electrochemistry of Single Nickelhydroxide Nanoparticles. *Chem. Commun.* **2016**, 52 (11), 2408–2411. <https://doi.org/10.1039/c5cc08796a>
- (29) Ying, Y.-L.; Ding, Z.; Zhan, D.; Long, Y.-T. Advanced Electroanalytical Chemistry at Nanoelectrodes. *Chem. Sci.* **2017**, 8, 3338–3348. <https://doi.org/10.1039/c7sc00433h>
- (30) Steegstra, P.; Ahlberg, E. In Situ pH Measurements with Hydrous Iridium Oxide in a Rotating Ring Disc Configuration. *J. Electroanal. Chem.* **2012**, 685, 1–7. <https://doi.org/10.1016/j.jelechem.2012.07.040>

- (31) El-Deen, E.; El-Giar, M.; Wipf, D. O. Microparticle-Based Iridium Oxide Ultramicroelectrodes for pH Sensing and Imaging. *J. Electroanal. Chem.* **2007**, 609 (2), 147-154. <https://doi.org/10.1016/j.jelechem.2007.06.022>
- (32) Marzouk, S. A. M. Improved Electrodeposited Iridium Oxide pH Sensor Fabricated on Etched Titanium Substrates. *Anal. Chem.* **2003**, 75 (6), 1258–1266. <https://doi.org/10.1021/ac0261404>
- (33) Debold, E. P.; Beck, S. E.; Warshaw, D. M. Effect of Low pH on Single Skeletal Muscle Myosin Mechanics and Kinetics. *American Journal of Physiology-Cell Physiology* **2008**, 295 (1), C173–C179. <https://doi.org/10.1152/ajpcell.00172.2008>